Correlating curvature to fault propagation in clay modeled transfer zones

Marcus Cahoj and Kurt J Marfurt, the University of Oklahoma*

Summary

Transfer zones are common hydrocarbon traps in extensional tectonic structures. A transfer zone is an area where one fault dies out and its slip is transferred to an adjacent fault. Transfer zones are commonly divided into three categories, convergent, divergent and synthetic, based on the dip of the faults. These zones can be quite subtle and little has been published on their signature in seismic data. Because of the complexity associated with transfer zones and their secondary faults, seismic attributes could prove to be valuable tools. Many of the secondary faults that occur in the proximity of a transfer zone may be below seismic resolution; however, these faults may provide an attribute expression that could aid the interpreter to infer their presence. In this study we compute the curvature of a suite of clay models of transfer zones. We then compare the curvature "attribute" to the underlying faults and fractures seen in the clay model. In this manner we provide a simple analogue model of how curvature, a measure of strain, is correlated to sub-seismic features of interest that can aid in the understanding and interpretation of transfer zone dynamics.

Introduction

Seismic curvature for fault imaging is a popular tool familiar to most geophysical interpreters. Curvature can be useful in delineating not only faults but also events that occur below the resolution of the seismic wavelet, such as fractures (Chopra and Marfurt, 2007). Events not clearly seen in the 3D seismic volume can still give a characteristic response with seismic attributes. Liao et al. (2013) used clay models of a strike slip fault in order to better understand secondary features such as fractures, splay shears and Riedel faults. These features were below seismic wavelet resolution however, with the help of the clay models Liao was able to predict these secondary features using seismic attributes characteristic responses in a 3D seismic data volume.

This paper analyzes curvature characteristics of the three types of transfer zones: (1) convergent transfer zone (Figure 1a) where the two main faults dip toward each other; divergent transfer zone (Figure 1b) where the two main faults dip in opposite directions; and synthetic transfer zones (Figure 1c) where the two main faults dip in the same direction (Morley et al., 1990). The three types of transfer zones were experimentally created using clay modeling (Paul and Mitra, 2013) and it was determined that fault propagation and transfer zone geometry was heavily reliant on the type of transfer zone being modeled. Using the clay modeled surfaces created by Paul and Mitra (2013) we try to correlate fault geometry of the three types of transfer zones with seismic curvature. We then compare the curvature and fractures of a clay modeled convergent transfer zone to the curvature and coherence response of a transfer zone in 3D seismic data in order to understand the appearance of subseismic faults and fractures on seismic attributes, such as curvature.

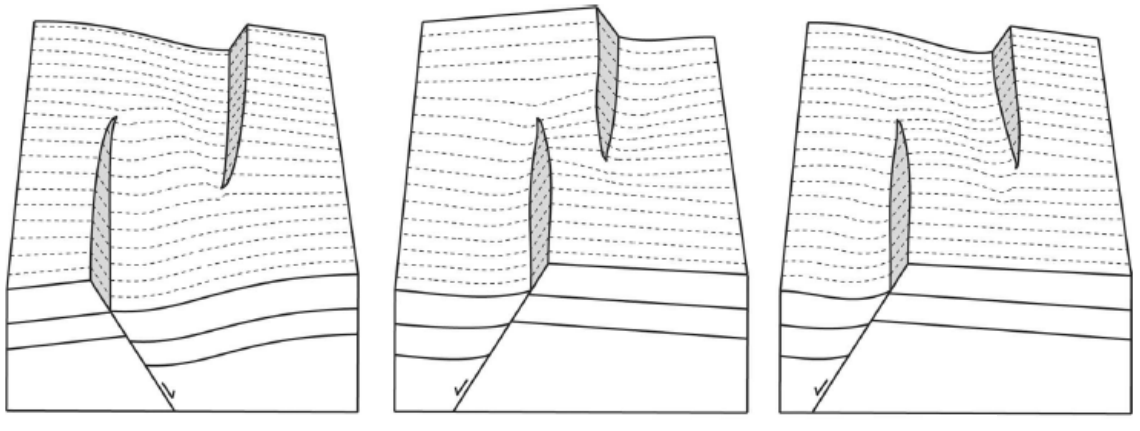

a b c

Figure 1. Schematic of the three types of transfer zones in rift systems. (a) Convergent transfer zone. (b) Divergent transfer zone. (c) Synthetic transfer zone (Morley et al., 1990; and Bose and Mitra, 2010).

DOI http://dx.doi.org/10.1190/segam2014-1338.1

Curvature of clay modeled transfer zones

Method

Clay Modeling

Paul and Mitra (2013) created clay models of transfer zones to illustrate the fault geometry and the corresponding fracture propagation of convergent, divergent and synthetic faults. They constructed two different density clay layers, one representative of the basement and the other representative of the overlying sedimentary sequences. The basement clay had a density of 1.85g/cm^3 with a thickness of 2.5 cm and the sedimentary clay had a density of 1.6 to 1.65g/cm^3 also with a thickness of 2.5 cm. In the bottom layer of clay, representative of the basement rock, pre-allocated fault cuts were made with a dip of 60 degrees. Then at a constant rate of 0.0005 cm/s extensional motion along the basement faults was generated. The process was repeated twice for each of the three types of transfer zones. The surface of the clay model was laser scanned at various stages of displacement to generate a point set. The point set had a density of 75 dots per inch, which allowed for faults with a minimum vertical separation of 0.4 mm to be mapped.

Computing Curvature

These scanned surfaces were imported into a commercial interpretation workstation where they were gridded and displayed as continuous surfaces for subsequent attribute analysis. Figure 2 shows the scanned surfaces with each colored layer being a different stage of displacement. Max and min curvature was computed for three different X and Y incremented bins in order to determine a realistic resolution. Max and min curvature overlay of Stage 5 is shown for an X and Y increment of 1, 2 and 5 bins (Figure 3). Incrementing by a value of 1 showed the best resolution, however it was qualitatively determined that an X and Y increment of 2 provided the most accurate analogue to long wavelength curvature values that are observed in seismic data.

Curvature was then computed for each of the five stages of the three transfer zones and co-rendered with fractures identified in the clay models, resulting in 15 images (Figure 4). The results from the clay models were used as an analogue to better understand a convergent transfer zone and associated relay ramp as seen in a 3D seismic curvature and coherence overlay created by Chopra and Marfurt (2010).

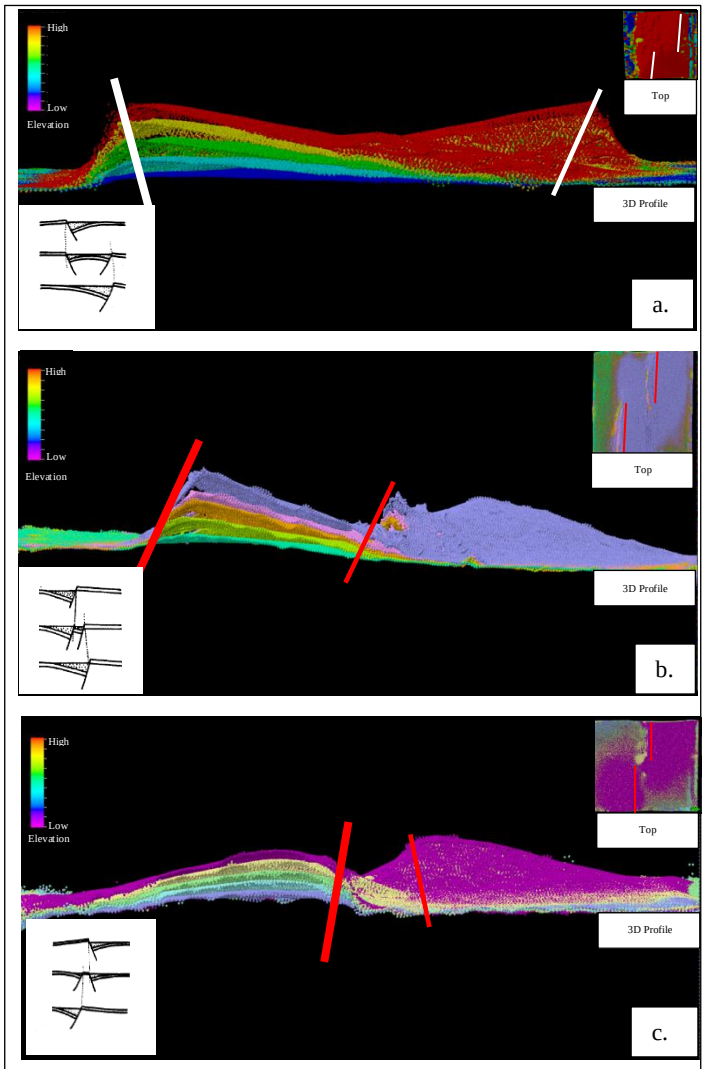

Figure 2. Images of the five stages of displacement for the convergent (a.), synthetic (b.) and divergent (c.) transfer zone. The faults are shown as red or white lines marked in a top and profile view.

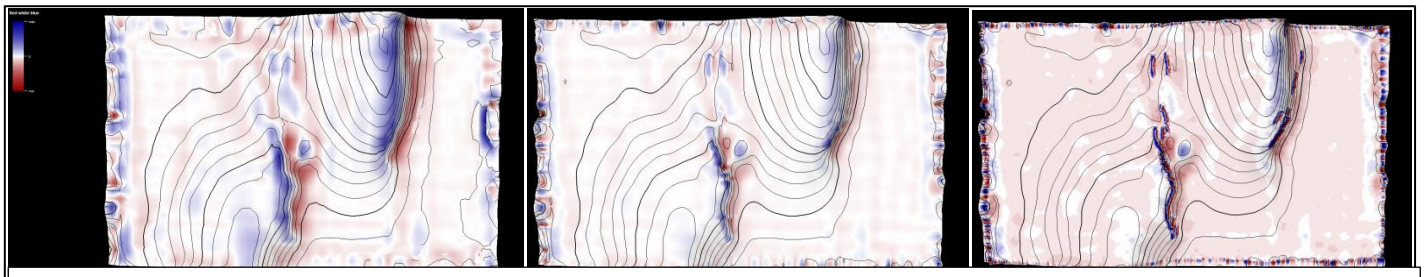

Figure 3. A synthetic fault during Stage 5 for the 3 increment sizes considered for generating curvature of the clay surface. (Left) X and Y increment of 5. (Center) X and Y increment of 2. (Right) X and Y increment of 1. It was determined that the X and Y increment of 2 most accurately replicates curvature seen in 3D seismic data volumes.

DOI http://dx.doi.org/10.1190/segam2014-1338.1

Curvature of clay modeled transfer zones

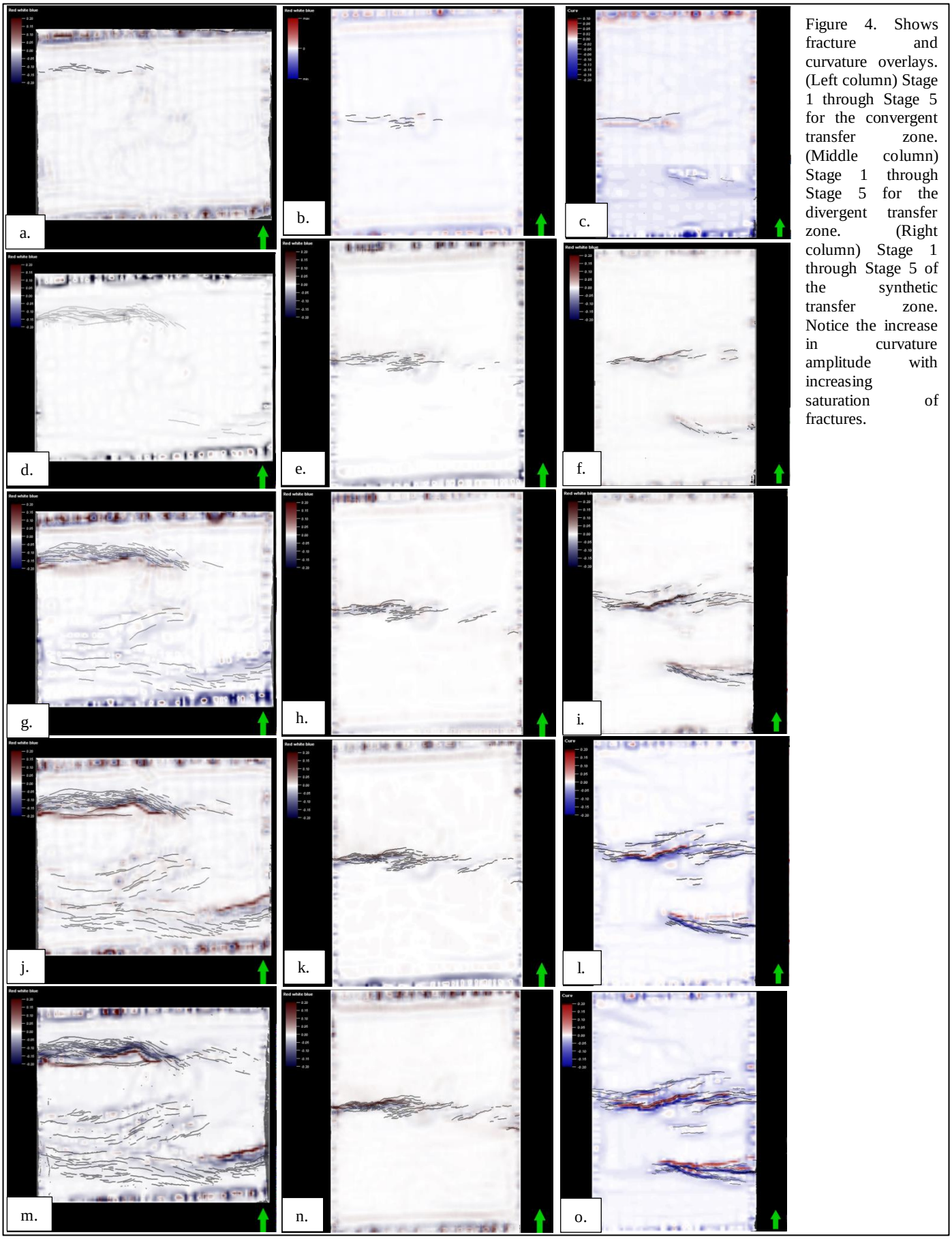

Figure 4. Shows fracture and curvature overlays. (Left column) Stage 1 through Stage 5 for the convergent transfer zone. (Middle column) Stage 1 through Stage 5 for the divergent transfer zone. (Right column) Stage 1 through Stage 5 of the synthetic transfer zone. Notice the increase in curvature amplitude with increasing saturation of fractures.

DOI http://dx.doi.org/10.1190/segam2014-1338.1

Results

It is visually apparent that there is a direct correlation between the number of fractures present in the clay models to the curvature of the clay models (Figure 4). Areas with higher curvature amplitude, a measure of strain, have more fractures. This can be seen by comparing Figure 4c to Figure 4o. In Figure 4c there are 9 fractures and only a weak corresponding curvature response. However, in Figure 4o there are 139 fractures identified and a very high amplitude in the curvature response. We can also see a spatial realtion to curvature and fractures. In the convergent transfer zone (Figure 4m) we see a curvature signature developing in between the main faults. We also can see evidence of a relay ramp forming when the fracture images are overlain. This visualization can be useful when applying the model to seismic data. In Figure 5a we see a convergent transfer zone in a 3D seismic curvature and cohernece overlay (circled in red). The faults and relay ramp are shown by green arrows. Applying what we have taken from the modeled convergent transfer zone we can conclude that the curvature signature connecting the two faults in Figure 5a can be attributed to fractures that are from a relay ramp and not an artifact within the data.

Conclusions

In conclusion, curvature computed over clay modeled transfer zones provides an analogue to help us better understand transfer zone geometry and related features, such as relay ramps. Furthermore, although curvature is a measure of strain it can be a useful tool in inferring fracture saturation and other subseismic features.

Acknowldgements

I would like to thank Debapriya Paul and Dr. Mitra for the use of their clay models and subsequent data. Also, thanks to sponsors of the AASPI Consortium for their finanacial support.

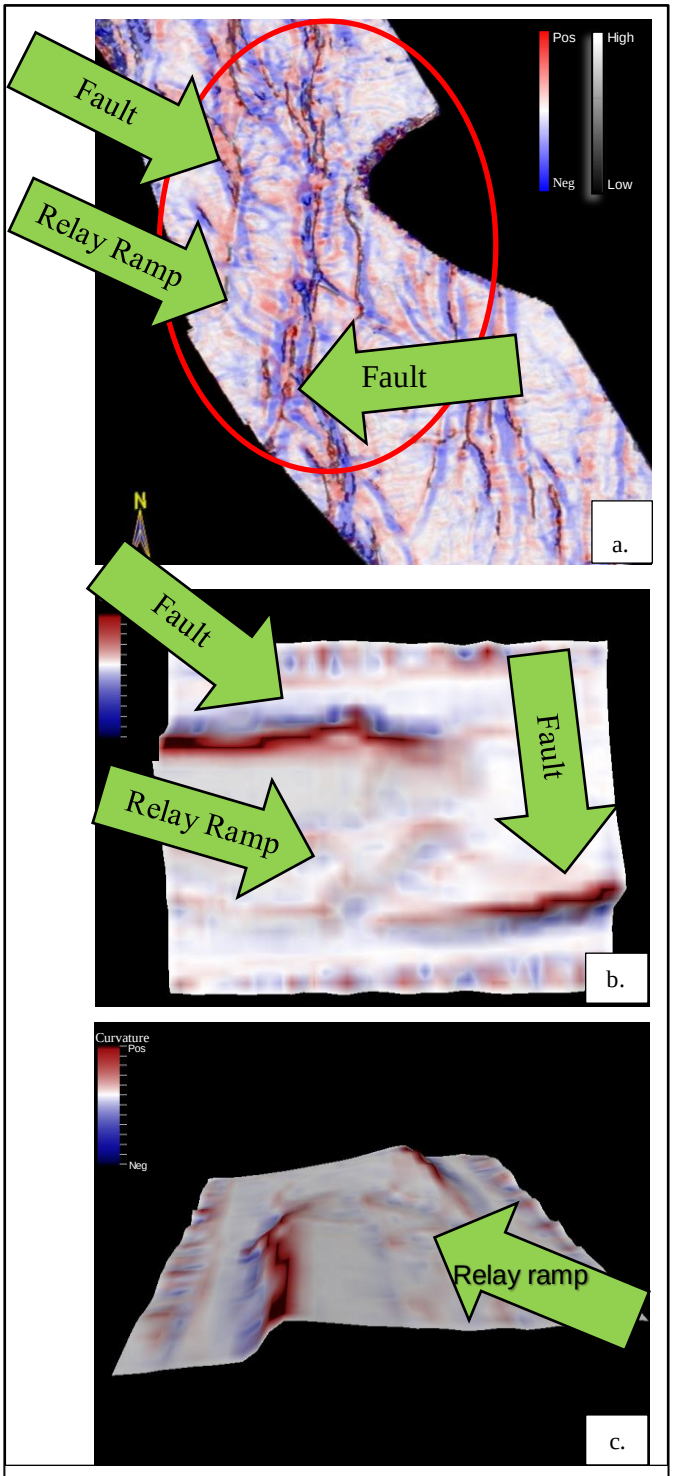

Figure 5. Coherence and curvature overlay (a.) showing a convergent transfer zone and relay ramp once thought to be an artifact (Modified from Chopra and Marfurt, 2010). (b.) Top view of the clay modeled transfer zone in curvature and signature of a relay ramp and associated fractures. (c.) The same image as (b.) but from a profile view.

DOI http://dx.doi.org/10.1190/segam2014-1338.1

http://dx.doi.org/10.1190/segam2014-1338.1

EDITED REFERENCES

Note: This reference list is a copy-edited version of the reference list submitted by the author. Reference lists for the 2014 SEG Technical Program Expanded Abstracts have been copy edited so that references provided with the online metadata for each paper will achieve a high degree of linking to cited sources that appear on the Web.

REFERENCES

Bose, S., and S. Mitra, 2010, Analog modeling of divergent and convergent transfer zones in listric normal fault systems: AAPG Bulletin, **94**, no. 9, 1425–1452, http://dx.doi.org/10.1306/01051009164.

Chopra, S., and K. J. Marfurt, 2007, Volumetric curvature-attribute applications for detection of fracture lineaments and their calibration, http://www.arcis.com/Satinder/PDFs/CURVATURE/Denver_GS_Arcis%20Article.pdf, accessed 21 March 2014.

Chopra, S., and K. J. Marfurt, 2010, Integration of coherence and volumetric curvature images: The Leading Edge, **29**, 1092–1107, http://dx.doi.org/10.1190/1.3485770.

Liao, Z., Z. Reches, K. J. Marfurt, and N. Gupta, 2013, Characterizing a fault-zone and associated fractures using lab experiments and attribute based seismic analysis: An example from the Woodford Shale, Anadarko basin, Oklahoma: Presented at the 83rd Annual International Meeting, SEG.

Morley, C. K., R. A. Nelson, T. L. Patton, and S. G. Munn, 1990, Transfer zones in the East African rift system and their relevance to hydrocarbon exploration in rifts: AAPG Bulletin, **74**, 1274–1253.

Paul, D., and S. Mitra, 2013, Experimental models of transfer zones in rift systems: AAPG Bulletin, **97**, no. 5, 759–780, http://dx.doi.org/10.1306/10161212105.